TAILORED FINITE POINT METHOD FOR FIRST ORDER WAVE EQUATION

ZHONGYI HUANG AND XU YANG

Abstract. Following the idea of the tailored finite point method proposed in [2, 7], a series of efficient numerical schemes are developed for the one dimensional scalar wave equation within various types of media. Stability and accuracy are analyzed and numerically verified. In particular we can obtain unconditionally stable implicit schemes that can be solved explicitly for boundary value problems. We can also deal with the propagation of discontinuity and highly oscillatory waves efficiently. The generalization to higher order schemes is straightforward.

1. Model and algorithm

Wave propagation is very popular in many physical fields, for example in fluid mechanics, geophysics and electromagnetism. In this paper we mainly concern the efficient computation of the following wave equation in one dimension,

$$u_t + a(x)u_x = 0, \tag{1.1}$$

within different types of media

(1) homogeneous media: $a(x)$ is constant;
(2) heterogenous media: $a(x)$ depends on the physical location;
(3) nonlinear waves: $u_t + f(u)_x = 0$.

There have existed many numerical methods for solving (1.1), for example the finite difference method and the finite element method. However none of them could efficiently deal with the cases when the initial condition contains either discontinuity (contact continuity) or high frequency component. For the propagation of the contact continuity, a common way is to make use of the ENO-scheme, for example [6]. For the computation of the high frequency wave propagation, asymptotic methods are mostly preferred, for example the review papers [1, 9] and the references therein. For the nonlinear wave propagation, the conservative numerical methods are usually used (*cf.* the book by LeVeque [8], and the references listed therein).

We aim at a uniform treatment of these wave propagation with an efficient method, so-called the *tailored finite point method*, recently developed for the numerical simulation of singular perturbation problems, high frequency wave propagation problems and interface problems [2, 3, 4, 5, 7]. The main idea underlying the method is to use the exact solution of the local approximate problem to construct the global approximate solution. For singular perturbation problems [3, 4, 5], without any prior knowledge of the boundary/interior layers, this method can

Key words and phrases. Tailored finite point method, wave equation, conservation laws, high frequency, discontinuity.

This work was partially supported by NSFC project No. 11071139, the National Basic Research Program of China under the grant 2011CB309705, Tsinghua University Initiative Scientific Research Program. This work was done during X.Y.'s visit to Tsinghua University, and he is grateful to their hospitality.

provide high accuracy even on the uniform coarse mesh $h \gg \varepsilon$, where ε is the small parameter in the singular perturbation problem. For the Helmholtz equation in one dimension [2], the method could give very good approximate solution on coarse meshes, and have uniform convergence in L^2 norm with respect to the wave number. For the interface problem [7], the method produces uniform convergence in energy norm even for the PDEs of mixed type.

Following the idea of these previous work, we develop some tailored finite point schemes for the first order convection problems in this paper. The new methods can deal with the discontinuous and high oscillatory initial conditions easily. Particularly we develop unconditionally stable implicit schemes for (1.1), which can be solved explicitly for boundary value problems. This is better than the traditional second order numerical schemes, say Lax-Wendroff and Beam-Warming, even for the smooth non-oscillatory initial conditions. We also obtain a TVD scheme for the conservation law by combing this method with some flux limiter. The extension to other types of wave propagation will be studied later.

The rest of this paper is organized as follows. In section 2, we present several tailored finite point schemes for wave propagations in homogeneous media. In section 3, we generalize the methods to the cases of heterogenous media and nonlinear waves. We give some concluding remarks in section 4.

2. Homogeneous media

Although it is easy to deal with the wave propagation in the homogeneous media, the numerical schemes for solving it will shed lights on those developed for the wave propagation in heterogeneous media and nonlinear waves later. Without loss of generality, we let $a(x) = a > 0$. Denote h as the mesh size of x and τ as the time step. The mesh grids are taken to be $x_j = x_0 + (j-1)h$, $t^n = n\tau$ where x_0 is the starting point. u_j^n is the numerical approximation of $u(t^n, x_j)$.

2.1. **Second order explicit numerical scheme.**

2.1.1. *Centered tailored finite point method (CTFPM).* First we derive an explicit scheme as follows,

$$u_j^{n+1} = \alpha_{-1} u_{j-1}^n + \alpha_0 u_j^n + \alpha_1 u_{j+1}^n. \tag{2.1}$$

We expect that the scheme (2.1) holds exactly for all the wave-formed functions in the space

$$V = \{v(x,t) \,|\, v(x,t) = c_1 + c_2 \exp(\mathrm{i}k_j(at-x)) + c_3 \exp(-\mathrm{i}k_j(at-x)), \quad \forall c_1, c_2, c_3 \in \mathbb{C}\}, \tag{2.2}$$

where k_j is the wave number in the j-th cell $[x_j, x_{j+1}]$ and 'i' is the imaginary unit $(= \sqrt{-1})$.

Denote the complex-valued initial condition by $u_0(x)$. Note that it can be rewritten as $u_0(x) = A_0(x)\exp\big(\mathrm{i}S_0(x)\big)$, where $A_0(x)$ and $S_0(x)$ are real-valued functions. By Taylor expansion, in the j-th cell,

$$S_0(x) = S_0(x_j) + S_0'(x_j)(x - x_j) + S_0''(\tilde{x}_j)(x - x_j)^2/2,$$

where $\tilde{x}_j \in [x_{j-1}, x_j]$.

To make the function in (2.2) give linear approximation for phase function at $t = 0$, we take $k_j = S_0'(x_j)$ in each cell, because the constant term coming from Taylor expansion of the phase function goes to c_3. Without further indication, we will use this choice of k_j for the schemes introduced later except the one dealing with high frequency initial condition in Section 3.1.2.

Taking the wave functions of $(c_1, c_2, c_3) = (1, 0, 0),\ (0, 1, 0),\ (0, 0, 1)$ in (2.2) gives

$$\begin{cases} 1 = \alpha_{-1} + \alpha_0 + \alpha_1, \\ \cos(k_j a\tau) = \alpha_{-1}\cos(k_j h) + \alpha_0 + \alpha_1 \cos(k_j h), \\ \sin(k_j a\tau) = \alpha_{-1}\sin(k_j h) - \alpha_1 \sin(k_j h). \end{cases} \tag{2.3}$$

Solving the above linear system (2.3) yields

$$\alpha_{-1} = \frac{\sin(k_j a\tau/2)\sin(k_j(a\tau + h)/2)}{\sin(k_j h/2)\sin(k_j h)}, \quad \alpha_1 = \frac{\sin(k_j a\tau/2)\sin(k_j(a\tau - h)/2)}{\sin(k_j h/2)\sin(k_j h)}, \tag{2.4}$$

$$\alpha_0 = 1 - \alpha_1 - \alpha_{-1}. \tag{2.5}$$

Stability analysis: We do the von Neumann analysis (discrete Fourier transform) to derive the stability condition. Suppose $u_j^n = U^n e^{\mathrm{i}\xi jh}$. Substituting it into the scheme (2.1), we get

$$U^{n+1} = U^n(\alpha_{-1}e^{-\mathrm{i}\xi h} + \alpha_0 + \alpha_1 e^{\mathrm{i}\xi h}),$$

which implies the amplification factor is

$$G = \alpha_{-1}e^{-\mathrm{i}\xi h} + \alpha_0 + \alpha_1 e^{\mathrm{i}\xi h}.$$

After calculations, the condition $|G| \le 1$ is equivalent to

$$1 - \cos^2(k_j h) - \cos(k_j h) + \cos k_j a\tau + \cos(\xi h) - \cos(k_j h)\cos(k_j a\tau)\cos(\xi h) \ge 0,$$

which is

$$(1 + \cos(\xi h))(1 - \cos(k_j h)\cos(k_j a\tau)) + (1 + \cos(k_j h))(\cos(k_j a\tau) - \cos(k_j h)) \ge 0.$$

Therefore $a\tau \le h$ will be sufficient to guarantee the stability of scheme (2.1).

Accuracy analysis: when $k_j a\tau,\ k_j h \ll 1$, the Taylor expansion shows that the scheme could be viewed as, after dropping the higher order terms $\mathcal{O}(h^3 + \tau^3)$,

$$u_j^{n+1} = u_j^n + \frac{a\tau}{2h}(u_{j-1}^n - u_{j+1}^n) + \frac{(a\tau)^2}{2h^2}(u_{j-1}^n - 2u_j^n + u_{j+1}^n),$$

which is the well-known Lax-Wendroff scheme. Therefore the scheme (2.1) has a second order accuracy.

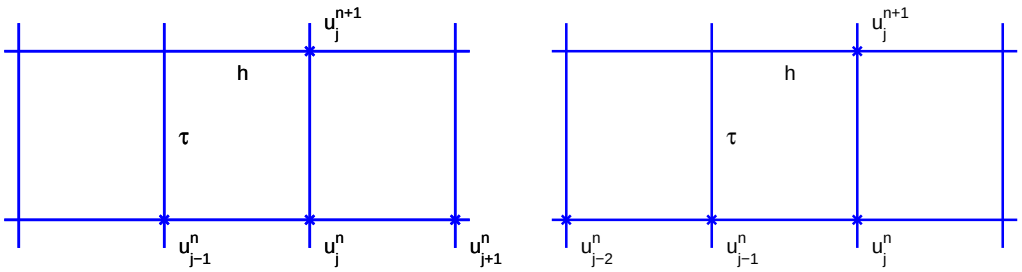

FIGURE 1. Stencils of the second order explicit tailored finite point schemes. Left: CTFPM; right: OSTFPM.

2.1.2. *One-sided tailored finite point method (OSTFPM).* To solve the boundary value problem with high order schemes, we need to consider the following type scheme

$$u_j^{n+1} = \alpha_{-2} u_{j-2}^n + \alpha_{-1} u_{j-1}^n + \alpha_0 u_j^n. \tag{2.6}$$

Taking the wave functions of $(c_1, c_2, c_3) = (1, 0, 0),\ (0, 1, 0),\ (0, 0, 1)$ in (2.2) yields

$$\begin{cases} 1 = \alpha_{-2} + \alpha_{-1} + \alpha_0, \\ \cos(k_j a\tau) = \alpha_{-2}\cos(2k_j h) + \alpha_{-1}\cos(k_j h) + \alpha_0, \\ \sin(k_j a\tau) = \alpha_{-2}\sin(2k_j h) + \alpha_{-1}\sin(k_j h), \end{cases}$$

which implies

$$\alpha_{-2} = \frac{\sin(k_j a\tau/2)\sin(k_j(a\tau - h)/2)}{\sin(k_j h/2)\sin(k_j h)}, \quad \alpha_{-1} = -\frac{\sin(k_j a\tau/2)\sin(k_j(a\tau - 2h)/2)}{\sin^2(k_j h/2)},$$
$$\alpha_0 = 1 - \alpha_{-2} - \alpha_{-1}.$$

Similar to the CTFPM, one knows that when $k_j a\tau,\ k_j h \ll 1$ the scheme is reduced to the Beam-Warming scheme, which has a second order accuracy and the stability condition $a\tau \le 2h$.

2.1.3. *Numerical study.* In this subsection, we present a numerical study of the above two numerical methods. Since CTFPM and OSTFPM have similar performances, we will focus on the accuracy study of CTFPM and only show that OSTFPM has a better stability condition.

Example 2.1. We take the wave speed $a = 1$, and the initial condition $u_0 = e^{-50x^2} e^{\mathrm{i}\sin(x)}$.

The analytical solution is $u(x, t) = e^{-50(x-t)^2} e^{\mathrm{i}\sin(x-t)}$.

The wave number is taken as $k_j = \cos(x_j)$. The comparison between the true solution and the numerical solution by CTFPM at $T = 1$ is shown in Figure 2, and the errors are given in Table 1. This verifies that the numerical convergence order is 2 for both the ℓ^∞ and ℓ^2 norms. The numerical solution by OSTFPM is given in Figure 3, which confirms that OSTFPM has a better CFL condition than CTFPM.

TABLE 1. Example 2.1, the ℓ^∞ and ℓ^2 errors for CTFPM.

(h, τ)	$(1/2^6, 1/2^7)$	$(1/2^7, 1/2^8)$	$(1/2^8, 1/2^9)$	$(1/2^9, 1/2^{10})$
ℓ^∞ error	4.26×10^{-2}	1.07×10^{-2}	2.67×10^{-3}	6.66×10^{-4}
ℓ^2 error	1.77×10^{-2}	4.50×10^{-3}	1.13×10^{-3}	2.82×10^{-4}

2.2. **Second order implicit numerical scheme.**

2.2.1. *Rectangular cell (RCTFPM).*

$$u_j^{n+1} = \alpha_{-1} u_{j-1}^{n+1} + \beta_{-1} u_{j-1}^n + \beta_0 u_j^n. \tag{2.7}$$

Taking the wave functions of $(c_1, c_2, c_3) = (1, 0, 0),\ (0, 1, 0),\ (0, 0, 1)$ in (2.2) gives

$$\begin{cases} 1 = \alpha_{-1} + \beta_{-1} + \beta_0, \\ \cos(k_j a\tau) = \alpha_{-1}\cos(k_j(a\tau + h)) + \beta_{-1}\cos(k_j h) + \beta_0, \\ \sin(k_j a\tau) = \alpha_{-1}\sin(k_j(a\tau + h)) + \beta_{-1}\sin(k_j h). \end{cases}$$

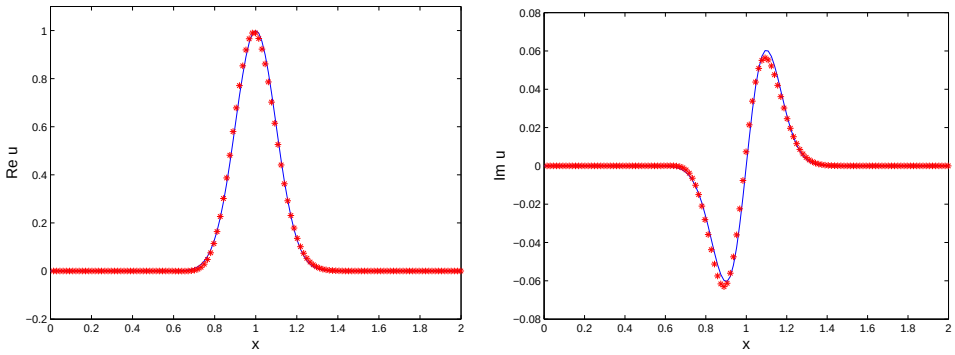

FIGURE 2. Example 2.1, the comparison between the true solution (solid) and the solution by CTFPM ('*') using $h = 1/2^6$, $\tau = 1/2^7$.

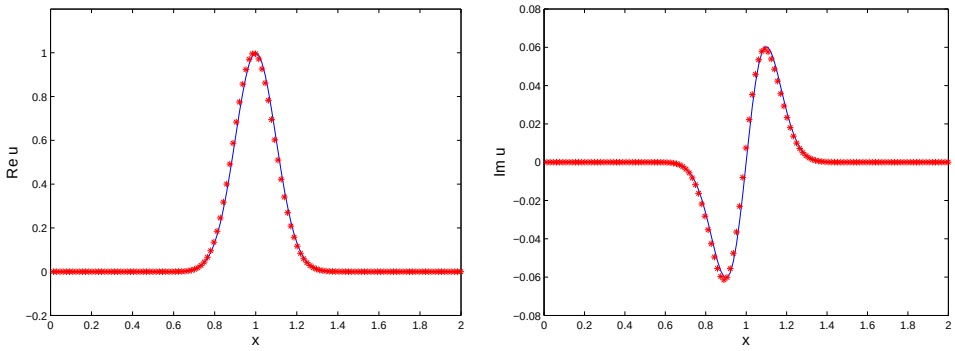

FIGURE 3. Example 2.1, the comparison between the true solution (solid line) and the solution by OSTFPM ('*') using $h = 1/2^6$, $\tau = 1/2^{5.5}$.

The above linear system shows that

$$\alpha_{-1} = \frac{\sin(k_j(a\tau - h)/2)}{\sin(k_j(a\tau + h)/2)}, \quad \beta_{-1} = 1, \quad \beta_0 = -\alpha_{-1}. \tag{2.8}$$

Stability analysis: the von Neumann analysis gives that,

$$U^{n+1}(1 - \alpha_{-1}e^{-i\xi h}) = U^n(-\alpha_{-1} + e^{-i\xi h}),$$

which implies the amplification factor is

$$G = \frac{-\alpha_{-1} + e^{-i\xi h}}{1 - \alpha_{-1}e^{-i\xi h}}.$$

Therefore $|G| = 1$, which means the scheme (2.7) is unconditionally stable.

Accuracy analysis: Taylor expansion shows that the scheme has a second order accuracy.

Remark 2.1. For the boundary value problem, the scheme (2.7) could be explicitly solved since the value at boundary mesh grid is already given.

2.2.2. *Parallelogram cell (PCTFPM).*

$$u_j^{n+1} = \alpha_{-1}u_{j-1}^{n+1} + \beta_{-1}u_{j-m-1}^n + \beta_0 u_{j-m}^n. \tag{2.9}$$

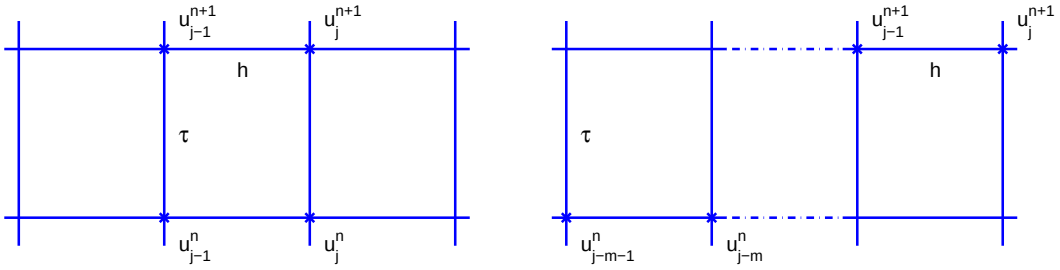

FIGURE 4. Stencils of the second order implicit tailored finite point schemes. Left: RCTFPM; right: PCTFPM.

Taking the wave functions of $(c_1, c_2, c_3) = (1, 0, 0),\ (0, 1, 0),\ (0, 0, 1)$ in (2.2) shows

$$\begin{cases} 1 = \alpha_{-1} + \beta_{-1} + \beta_0, \\ \cos(k_j a\tau) = \alpha_{-1}\cos(k_j(a\tau + h)) + \beta_{-1}\cos(k_j(m+1)h) + \beta_0\cos(mh), \\ \sin(k_j a\tau) = \alpha_{-1}\sin(k_j(a\tau + h)) + \beta_{-1}\sin(k_j(m+1)h) + \beta_0\sin(mh), \end{cases}$$

which implies

$$\alpha_{-1} = \frac{\sin(k_j(a\tau - (m+1)h)/2)}{\sin(k_j(a\tau - (m-1)h)/2)}, \quad \beta_{-1} = 1, \quad \beta_0 = -\alpha_{-1}.$$

Similarly it is easy to see that the scheme is unconditionally stable by the von Neumann analysis. In the following subsection we will show that the scheme could provide the machine accurate solution by choosing appropriate integer m for the homogeneous wave equation.

2.2.3. *Numerical study.*

Example 2.2. Take the wave speed $a = 1$, and the initial condition as $u_0 = e^{-50x^2} e^{\mathrm{i}\sin(x)}$.

The analytical solution is $u(x, t) = e^{-50(x-t)^2} e^{\mathrm{i}\sin(x-t)}$.

We take the wave number $k_j = \cos(x_j)$. The comparison between the true solution and the numerical solution by RCTFPM at $T = 1$ is shown in Figure 5, and the errors are given in Table 2. This verifies that the numerical convergence order is 2 for both the ℓ^∞ and ℓ^2 norms. The numerical solution by PCTFPM is given in Figure 6, and the ℓ^∞ error is 1.73×10^{-18}, which is the machine accuracy.

TABLE 2. Example 2.2, the ℓ^∞ and ℓ^2 errors for RCTFPM.

(h, τ)	$(1/2^6, 1/2^5)$	$(1/2^7, 1/2^6)$	$(1/2^8, 1/2^7)$	$(1/2^9, 1/2^8)$
ℓ^∞ error	8.37×10^{-2}	2.13×10^{-2}	5.29×10^{-3}	1.32×10^{-3}
ℓ^2 error	3.40×10^{-2}	8.85×10^{-3}	2.23×10^{-3}	5.59×10^{-4}

2.3. **Propagation of high frequency wave and discontinuity.** The parallelogram celled tailored finite point method (PCTFPM) could be used for computing the propagation of high frequency wave and discontinuity efficiently.

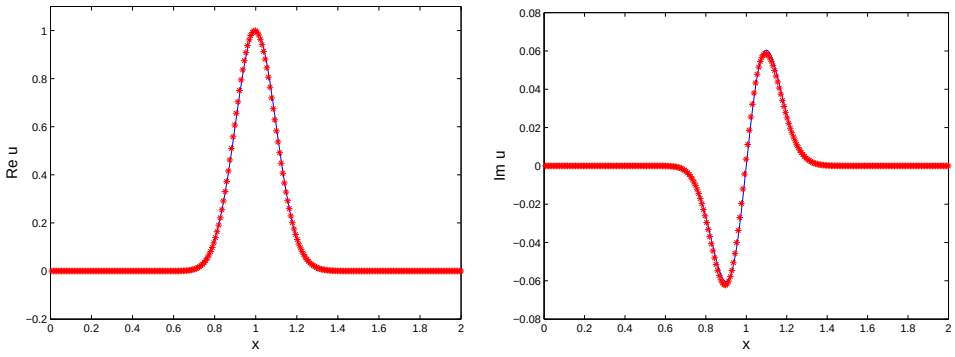

FIGURE 5. Example 2.2, the comparison between the true solution (solid line) and the solution by RCTFPM ('*') using $h = 1/2^7$, $\tau = 1/2^6$.

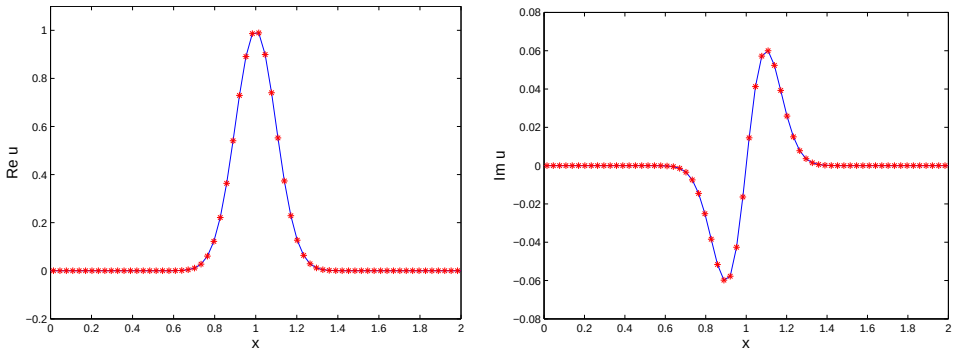

FIGURE 6. Example 2.2, the comparison between the true solution (solid line) and the solution by PCTFPM ('*') using $h = 1/2^5$, $\tau = 1/2^3$ and $m = 4$.

TABLE 3. Example 2.3, the ℓ^∞ errors between the true solution and the reconstructed solution by PCTFPM.

(h, τ)	$(1/2^6, 1/2^4)$	$(1/2^7, 1/2^5)$	$(1/2^8, 1/2^6)$	$(1/2^9, 1/2^7)$
ℓ^∞ error	9.82×10^{-4}	2.65×10^{-4}	6.83×10^{-5}	1.73×10^{-5}

2.3.1. *Computation of high frequency wave propagation.*

Example 2.3. We choose the wave speed $a = 1$, and the initial condition $u_0 = e^{-50x^2} e^{\mathrm{i}x/\varepsilon}$.

The analytical solution is $u(x,t) = e^{-50(x-t)^2} e^{\mathrm{i}(x-t)/\varepsilon}$.

We take $\varepsilon = 0.001$ and the wave number $k_j = 1/\varepsilon$. The numerical solution by PCTFPM is given in Figure 7, and the ℓ^∞ error on the gird points is 1.11×10^{-15}, which is the machine error. The wave field reconstructed in one cell using linear interpolation for phase function is shown in Figure 8. We can see that our method has high accuracy even we only use one mesh point in about two wavelength. The ℓ^∞ errors between the true solution and the reconstructed solution by PCTFPM are shown in Table 3 for different ε's, which shows that the convergence order is 1.94.

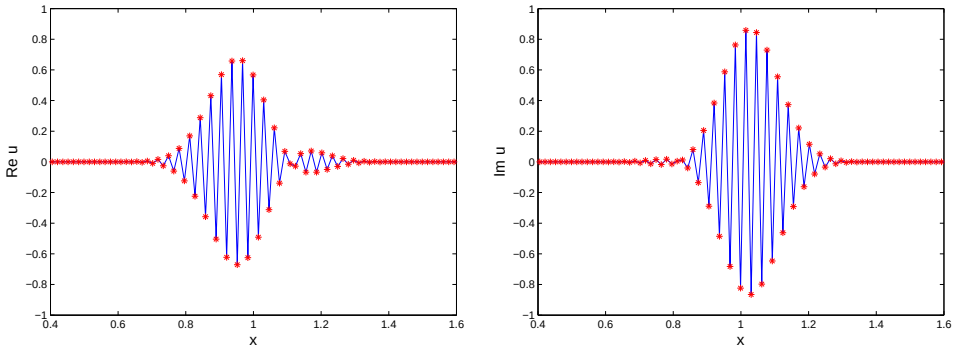

FIGURE 7. Example 2.3, the comparison between the true solution (solid line) and the solution by PCTFPM ('*') using $h = 1/2^6$, $\tau = 1/2^4$ and $m = 4$.

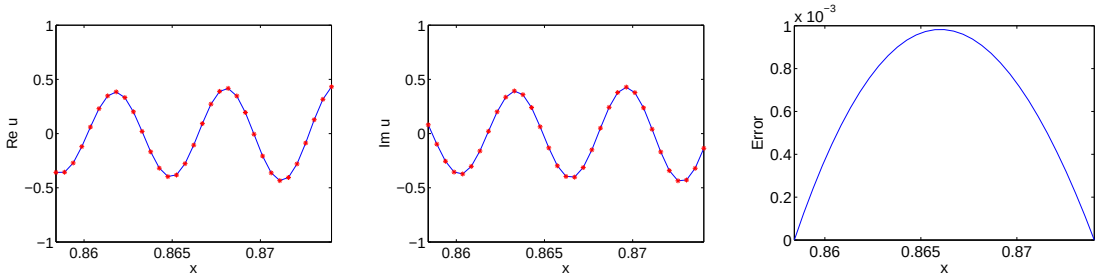

FIGURE 8. Example 2.3, the comparison between the true solution (solid line) and the solution by PCTFPM ('*') reconstructed in *one* mesh cell $[0.8584, 0.8740]$ using $h = 1/2^6$, $\tau = 1/2^4$ and $m = 4$, *i.e.* we only use one mesh point in about two wavelength.

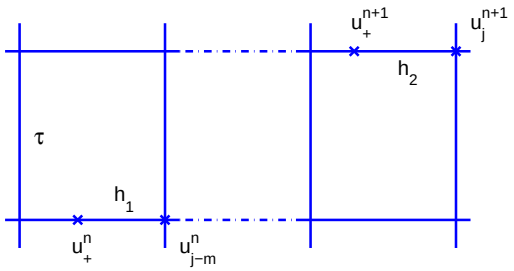

FIGURE 9. Stencil of the PCTFPM at the presence of discontinuity.

2.3.2. *Computation of discontinuity propagation.* In this case, we need to take care of special cells crossing the interface. Assume the discontinuity locates at u_+^n, u_+^{n+1} for two successive time steps (*cf.* Fig. 9), then

$$u_j^{n+1} = \alpha_{-1} u_+^{n+1} + \beta_{-1} u_+^n + \beta_0 u_{j-m}^n. \tag{2.10}$$

Taking the wave functions of $(c_1, c_2, c_3) = (1, 0, 0),\ (0, 1, 0),\ (0, 0, 1)$ in (2.2) yields

$$\begin{cases} 1 = \alpha_{-1} + \beta_{-1} + \beta_0, \\ \cos(k_j a\tau) = \alpha_{-1}\cos(k_j(a\tau + h_1)) + \beta_{-1}\cos(k_j(mh + h_2)) + \beta_0\cos(mh), \\ \sin(k_j a\tau) = \alpha_{-1}\sin(k_j(a\tau + h_1)) + \beta_{-1}\sin(k_j(mh + h_2)) + \beta_0\sin(mh). \end{cases}$$

Solving the above linear system yields

$$\begin{aligned} \alpha_{-1} &= \frac{\sin(k_j(a\tau - mh)/2)\sin(k_j(a\tau - mh - h_2)/2)}{\sin(k_j(a\tau - mh + h_1)/2)\sin(k_j(a\tau - mh + h_1 - h_2)/2)}, \\ \beta_{-1} &= \frac{\sin(k_j h_1/2)\sin(k_j(a\tau - mh)/2)}{\sin(k_j h_2/2)\sin(k_j(a\tau - mh + h_1 - h_2)/2)}, \\ \beta_0 &= 1 - \alpha_{-1} - \beta_{-1}. \end{aligned}$$

Example 2.4. The wave speed $a = 1$, and the discontinuous initial condition is taken as $u_0 = \mathrm{sign}(x)e^{-50x^2}e^{\mathrm{i}x/\varepsilon}$, where

$$\mathrm{sign}(x) = \begin{cases} 1 & x > 0, \\ 0 & x = 0, \\ -1 & x < 0. \end{cases}$$

The analytical solution is $u(x,t) = \mathrm{sign}(x - t)e^{-50(x-t)^2}e^{\mathrm{i}(x-t)/\varepsilon}$.

We take $\varepsilon = 0.2$ and the wave number $k_j = 1$. The numerical solution by PCTFPM is given in Figure 10, and the ℓ^∞ error is 1.73×10^{-18}.

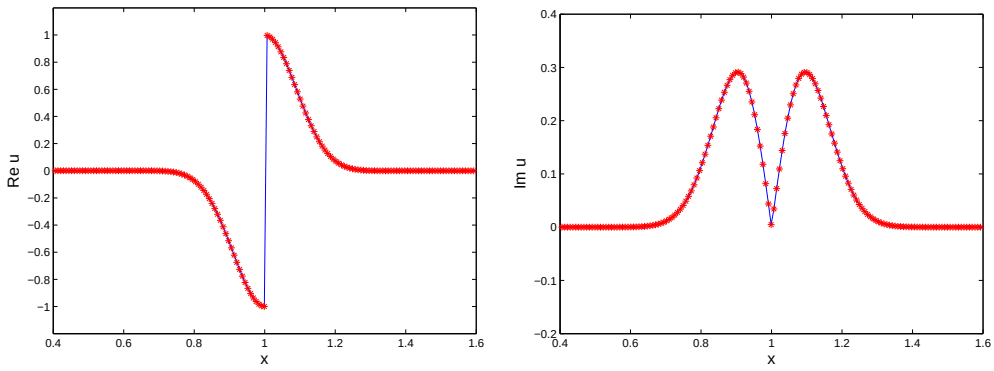

FIGURE 10. Example 2.4, the comparison between the true solution (solid line) and the solution by PCTFPM ('*') using $h = 1/2^7$, $\tau = 1/2^6$ and $m = 2$.

3. Heterogeneous media and nonlinear wave

3.1. **Linear problem with variable coefficient.** The schemes introduced in Sections 2.1.1, 2.1.2, 2.2.1 can be generalized to the heterogeneous wave propagation. In the following we will focus on two cases: (1) General initial condition. (2) High frequency initial condition. The difference lies in that, one has to update the wave number "k" in each time step for the second case.

TABLE 4. Example 3.1, the ℓ^∞ and ℓ^2 errors for CTFPM.

(h,τ)	$(1/2^5,1/2^8)$	$(1/2^6,1/2^9)$	$(1/2^7,1/2^{10})$	$(1/2^8,1/2^{11})$
ℓ^∞ error	1.36×10^{-1}	3.40×10^{-2}	6.43×10^{-3}	1.67×10^{-3}
ℓ^2 error	7.38×10^{-2}	1.87×10^{-2}	3.98×10^{-3}	9.90×10^{-4}

3.1.1. *General initial condition.* One can approximate the propagation speed $a(x)$ by using the piecewise constant function. In Section 2.1.1, the coefficients (2.4) are updated as

$$\alpha_{-1}=\frac{\sin(k_ja_j\tau/2)\sin(k_j(a_j\tau+h)/2)}{\sin(k_jh/2)\sin(k_jh)},\quad \alpha_1=\frac{\sin(k_ja_j\tau/2)\sin(k_j(a_j\tau-h)/2)}{\sin(k_jh/2)\sin(k_jh)},$$
$$\alpha_0=1-\alpha_1-\alpha_{-1},$$

and in Section 2.2.1, the coefficients (2.8) are updated as

$$\alpha_{-1}=\frac{\sin(k_j(a_j\tau-h)/2)}{\sin(k_j(a_j\tau+h)/2)},\quad \beta_{-1}=1,\quad \beta_0=-\alpha_{-1},$$

where $a_j=a(x_j)$.

Example 3.1. The wave speed $a(x)=\pi+x$, and the initial condition is taken as $u_0(x)=e^{-50x^2}e^{\mathrm{i}\sin(x)}$.

The analytical solution is $u(x,t)=e^{-50((\pi+x)e^{-t}-\pi)^2}e^{\mathrm{i}\sin((\pi+x)e^{-t}-\pi)}$.

The wave number $k_j=\cos(x_j)$. The comparison between the true solution and the numerical solution by CTFPM at $T=0.5$ is shown in Figure 11, and the errors are given in Table 4. This verifies that the numerical convergence order is 1.94 and 2.09 for the ℓ^∞ and ℓ^2 norms separately. The comparison between the true solution and the numerical solution by RCTFPM at $T=0.5$ is shown in Figure 12, and the errors are given in Table 5. This verifies that the numerical convergence order is 2.09 and 2.03 for both the ℓ^∞ and ℓ^2 norms separately.

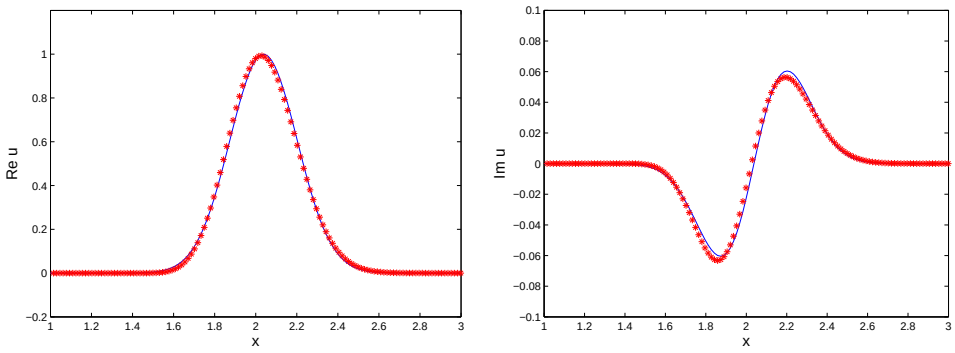

FIGURE 11. Example 3.1, the comparison between the true solution (solid) and the solution by CTFPM ('*') using $h=1/2^6$, $\tau=1/2^9$.

3.1.2. *High frequency initial condition.* We consider the WKB initial condition

$$u_0(x)=A_0(x)e^{\mathrm{i}S_0(x)/\varepsilon},$$

where ε is a small parameter that characterizes high frequency. The direct computation of (1.1) by finite difference method requires mesh size to be $o(\varepsilon)$ to obtain good accuracy.

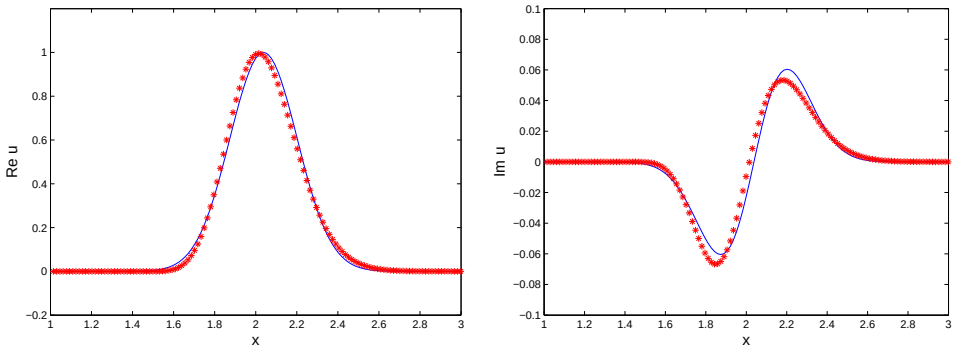

FIGURE 12. Example 3.1, the comparison between the true solution (solid) and the solution by RCTFPM ('*') using $h = 1/2^6$, $\tau = 1/2^7$.

TABLE 5. Example 3.1, the ℓ^∞ and ℓ^2 errors for RCTFPM.

(h, τ)	$(1/2^5, 1/2^6)$	$(1/2^6, 1/2^7)$	$(1/2^7, 1/2^8)$	$(1/2^8, 1/2^9)$
ℓ^∞ error	2.32×10^{-1}	6.29×10^{-2}	1.28×10^{-2}	3.17×10^{-3}
ℓ^2 error	1.29×10^{-1}	3.51×10^{-2}	7.63×10^{-3}	1.97×10^{-3}

We approximate the propagation wave speed $a(x)$ by piecewise linear function, *i.e.* in the j-th cell,

$$a(x) \approx b_j + c_j x, \quad \text{where} \quad b_j = \frac{a(x_{j-1})x_j - a(x_j)x_{j-1}}{h} \quad \text{and} \quad c_j = \frac{a(x_j) - a(x_{j-1})}{h}.$$

Then at $t^n = n\tau$, the local solution in the j-th cell can be approximated by

$$u(x_j, t^n) = A_0(y_j^n) \exp\big(\mathrm{i} S_0(y_j^n)/\varepsilon\big),$$

where $y_j^n = \big((b_j + c_j x_j)e^{-c_j t^n} - b_j\big)/c_j$. Similar to the argument given in Section 2.1.1 for the choice of k, Taylor expansion of phase function implies that the local wave number k_j^n should be updated in time according to

$$k_j^n = S_0'(y_j^n) e^{-c_j t^n}/\varepsilon.$$

Therefore in Section 2.2.1, the coefficients (2.8) are updated as

$$\alpha_{-1}^n = \frac{\sin(k_j^n(a_j\tau - h)/2)}{\sin(k_j^n(a_j\tau + h)/2)}, \quad \beta_{-1}^n = 1, \quad \beta_0^n = -\alpha_{-1}^n,$$

where $a_j = a(x_j)$.

Example 3.2. In this example, we take the wave speed $a(x) = 0.5 + x$, and the initial datum

$$u_0(x) = e^{-200x^2} e^{\mathrm{i}\sin(x)/\varepsilon}, \tag{3.1}$$

with $\varepsilon = 0.01$.

The comparison between the true solution and the numerical solution by RCTFPM at $T = 0.25$ is shown in Figure 13, and the errors are given in Table 6. Our method is much better than the traditional finite difference scheme.

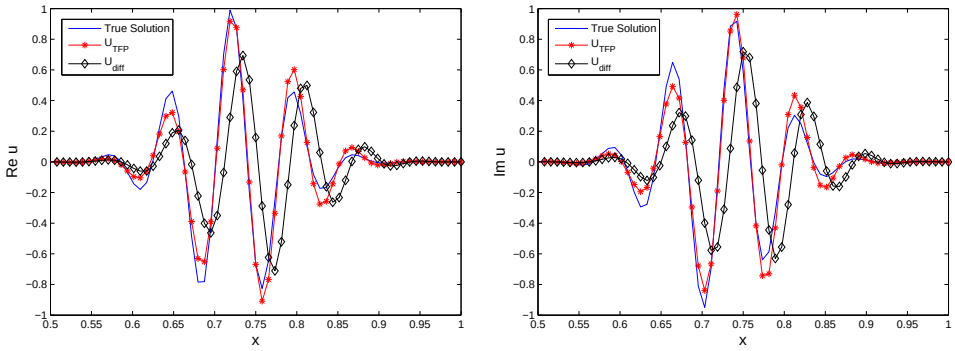

FIGURE 13. Example 3.2, the comparison between the true solution (solid line), the solution by RCTFPM ('*') and the solution by Lax-Wendroff scheme ('◇') using $h = 1/2^6$, $\tau = 1/2^7$.

TABLE 6. Example 3.2, the ℓ^∞ and ℓ^2 errors for RCTFPM.

(h, τ)	$(1/2^6, 1/2^7)$	$(1/2^7, 1/2^8)$	$(1/2^8, 1/2^9)$	$(1/2^9, 1/2^{10})$
ℓ^∞ error	5.83×10^{-1}	1.59×10^{-1}	3.95×10^{-2}	9.84×10^{-3}
ℓ^2 error	7.30×10^{-1}	1.88×10^{-1}	4.56×10^{-2}	1.13×10^{-2}

Example 3.3. In this example, we take the wave speed as a nonlinear function $a(x) = \frac{2x+\cos x}{2-\sin x}$, and the initial datum

$$u_0(x) = e^{-10(2x+\cos x)^2} e^{\mathrm{i}\sin(2x+\cos x)/\varepsilon}, \tag{3.2}$$

with $\varepsilon = 0.02$.

The comparison between the true solution and the numerical solution by RCTFPM at $T = 0.4$ is shown in Figure 14, and the errors are given in Table 7. It is clear that our method is much better than the traditional finite difference scheme.

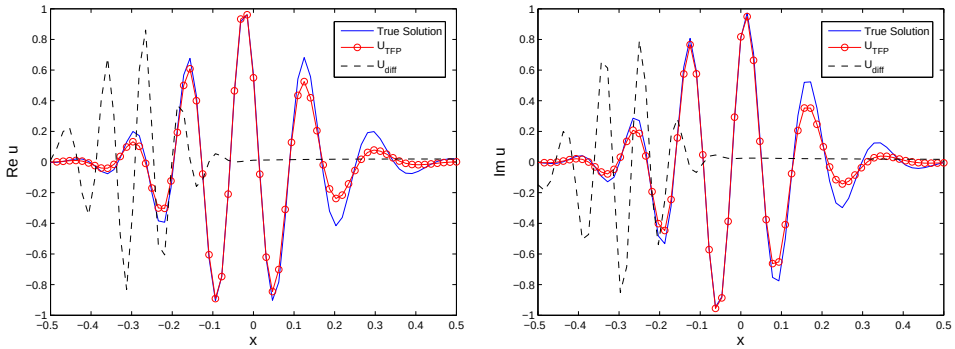

FIGURE 14. Example 3.3, the comparison between the true solution (solid line), the solution by RCTFPM ('o') and the solution by Lax-Wendroff scheme (dash line) using $h = 1/2^6$, $\tau = 1/2^7$.

3.2. **TFPM for conservation laws.** Based on the TFPM schemes and with the help of some flux limiters, we can easily get the TVD methods for the initial value problem of conservation

TABLE 7. Example 3.3, the ℓ^∞ and ℓ^2 errors for RCTFPM.

(h,τ)	$(1/2^6,1/2^6)$	$(1/2^7,1/2^7)$	$(1/2^8,1/2^8)$	$(1/2^9,1/2^9)$
ℓ^∞ error	4.49×10^{-1}	1.14×10^{-1}	2.80×10^{-2}	6.98×10^{-3}
ℓ^2 error	3.96×10^{-1}	1.05×10^{-1}	2.65×10^{-2}	6.64×10^{-3}

laws,

$$\begin{cases} u_t + f(u)_x = 0, & x\in\mathbb{R},\ t>0,\\ u|_{t=0} = u_0(x), & x\in\mathbb{R}. \end{cases} \tag{3.3}$$

For clarity we present the TVD method for the Burgers' equation in the following example.

Example 3.4. We take $f(u)=u^2/2$. The initial condition is taken as

$$u_0 = \begin{cases} 1 & 0.4\le x\le 0.6,\\ 0 & \text{elsewhere.}\end{cases}$$

We first describe the TVD method based on the CTFPM and the Godunov methods with the help of the van Leer flux limiter. The conservative scheme is written as

$$u_j^{n+1} = u_j^n - \lambda\left(g^n_{j+\frac12} - g^n_{j+\frac12}\right),$$

where $\lambda=\tau/h$. The flux $g^n_{j+\frac12}$ is given by

$$g^n_{j+\frac12} = \frac{(u_j^n)^2}{2} + \phi_j^n\left(-\frac{1}{\lambda}(\alpha_j^n u^n_{j+1} - \beta_j^n u_j^n) - \frac{(u^n_{j+1}+u_j^n)u_j^n}{2}\right),$$

where

$$\alpha_j^n = \frac{\sin\Big((u^n_{j+1}+u_j^n)\tau/4\Big)\sin\Big(\big((u^n_{j+1}+u_j^n)\tau/2-h\big)/2\Big)}{\sin(h/2)\sin(h)},$$

$$\beta_j^n = \frac{\sin\Big((u^n_{j+1}+u_j^n)\tau/4\Big)\sin\Big(\big((u^n_{j+1}+u_j^n)\tau/2+h\big)/2\Big)}{\sin(h/2)\sin(h)},$$

and the van Leer flux limiter ϕ_j^n is taken as

$$\phi_j^n = \frac{\theta_j^n + \left|\theta_j^n\right|}{1+\left|\theta_j^n\right|}, \quad \text{where} \quad \theta_j^n = \frac{u_j^n - u^n_{j-1}}{u^n_{j+1}-u_j^n}.$$

The true solution at $T=1$ is given by

$$u(t,x) = \begin{cases} 0 & x<0.4,\\ \frac{x-0.4}{T} & 0.4\le x<0.4+\frac{2\sqrt{T}}{\sqrt{10}},\\ 0 & 0.4+\frac{2\sqrt{T}}{\sqrt{10}}\le x.\end{cases}$$

The comparison between the true solution and the numerical solution by CTFPM using the van Leer flux limiter at $T=1$ is shown in Figure 15, and the ℓ^1 errors are given in Table 8. This shows that the numerical convergence order is 2.16 for the ℓ^1 norm.

TABLE 8. Example 3.4, the ℓ^1 errors for CTFPM.

(h,τ)	$(1/2^7, 1/2^8)$	$(1/2^8, 1/2^9)$	$(1/2^9, 1/2^{10})$	$(1/2^{10}, 1/2^{11})$
ℓ^1 error	2.70×10^{-3}	4.24×10^{-4}	1.17×10^{-4}	2.83×10^{-5}

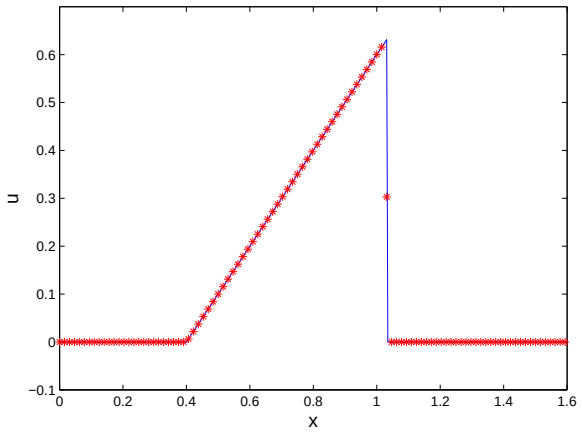

FIGURE 15. Example 3.4, the comparison between the true solution (solid) and the solution by CTFPM ('*') using $h = 1/2^8$, $\tau = 1/2^9$ with the van Leer flux limiter.

4. Conclusion

In this paper, following the idea of the tailored finite point method proposed in [2, 7], a series of TFPM schemes are developed for the one dimensional wave equation within various types of media. Stability and accuracy are analyzed and numerically verified. Especially we get unconditionally stable implicit schemes which can be solved explicitly for the boundary value problems. Our new method can deal with the propagation of discontinuity and highly oscillatory waves efficiently. We also extend our schemes for conservation laws with the help of the flux limiter technique. The extension to other types of wave propagation problems will be investigated later.

References

1. B. Engquist and O. Runborg, *Computational high frequency wave propagation*, Acta Numerica, **12** (2003): 181-266.
2. H. Han and Z. Huang, *A tailored finite point method for the Helmholtz equation with high wave numbers in heterogeneous medium*, J. Comput. Math, **26** (2008): 728-739.
3. H. Han and Z. Huang, *Tailored finite point method for a singular perturbation problem with variable coefficients in two dimensions*, J. Sci. Comput., **41** (2009): 200-220.
4. H. Han and Z. Huang, *Tailored finite point method for steady-state reaction-diffusion equation*, Commun. Math. Sci., **8** (2010): 887-899.
5. H. Han, Z. Huang and B. Kellogg, *A Tailored finite point method for a singular perturbation problem on an unbounded domain*, J. Sci. Comput. **36** (2008): 243-261.
6. A. Harten, *ENO schemes with subcell resolution*, J. Comput. Phys., **83** (1989): 148-184.
7. Z. Huang, *Tailored finite point method for the interface problem*, Netw. Heterog. Media, **4** (2009): 91-106.
8. R.J. LeVeque, **Numerical Methods for Conservation Laws**, Birkhäuser Verlag, Boston, 1992.
9. O. Runborg, *Mathematical models and numerical methods for high frequency waves*, Commun. Comput. Phys., **2** (2007): 827–880.

(Z. Huang) Department of Mathematical Sciences, Tsinghua University, Beijing 100084, China

E-mail address: zhuang@math.tsinghua.edu.cn

(X. Yang) Program in Applied and Computational Mathematics, Princeton University, Princeton, NJ 08544, USA. Current address: Department of Mathematics, Courant Institute of Mathematical Sciences, New York University, New York, NY 10012, USA

E-mail address: xuyang@cims.nyu.edu